geomagnetic latitude to those at 46 degrees was estimated about 0.28. This ratio means the attenuation of the electric field from 46° to 24° geomagnetic latitude in the nightside.

Kikuchi et al. [1978] estimated the geometrical attenuation of penetration electric field from polar region to the equator with decreasing latitude. Our observational result of attenuation of DP2 electric field amplitude in the nightside is comparable to their result.

In May, 2009, the third FM-CW radar was installed at near equatorial station at Manila, Philippine. By using this new radar data, similar comparison of amplitude attenuation will be extended to the equatorial region.

## References

1. Kikuchi, T., T. Araki, H. Maeda, and K. Maekawa, Transmission of polar electric fields to the equator, Nature, 273, 650-651, 1978.
2. Nishida, A., Geomagnetic DP2 fluctuations and associated magnetospheric phenomena, *J. Geophys. Res., 73,* 1795-1803, 1968a.
3. Nishida A., Coherence of geomagnetic DP2 fluctuations with interplanetary magnetic field variations, *J. Geophys. Res., 73*, 5549-5559, 1968b.
4. Sibeck D. G., K. Takahashi, K. Yumoto, and G. D. Reeves, Concerning the origin of signatures in dayside equatorial ground magnetograms, *J. Geophys. Res., 103,* 6763-6769, 1998.

# OBSERVATIONS OF THE IONOSPHERIC DISTURBANCES AND GEOMAGNETIC PULSATIONS IN THE FAR-EASTERN RUSSIA AND JAPAN
# НАБЛЮДЕНИЯ ИОНОСФЕРНЫХ ВОЗМУЩЕНИЙ И ГЕОМАГНИТНЫХ ПУЛЬСАЦИЙ НА ДАЛЬНЕМ ВОСТОКЕ РОССИИ И ЯПОНИИ

[1]Shiokawa, K., R. Nomura, and Y. Otsuka B. M. [2]Shevtsov
[1]Solar-Terrestrial Environment Laboratory, Nagoya University, Japan
[2]Institute of Cosmophysical Research and Radio Wave Propagation, Far Eastern Branch of the Russian Academy of Sciences, Russian Federation

*Мы проводили стандартные измерения среды геокосмоса на широтах Дальнего Востока России и Японии с 2007 года используя панорамные камеры свечения атмосферы и индукционных магнитометров в сотрудничестве с Институтом Космофизических Исследований и Распространения Радиоволн, Дальневосточное Отделение Российской Академии Наук. С помощью наблюдений с получением изображений свечения атмосферы на 630 нм, в ночное время часто регистрируются средне масштабные перемещающиеся ионосферные возмущения (MSTIDs). MSTIDs в основном распространяются в южном направлении над Японией, в то время как над Дальнем Востоком России некоторые MSTIDs распространяются в северном направлении, указывая на то, что направление распространения имеет широтную разницу. Индукционные магнитометры измеряют геомагнитные пульсации Pc1, которые распространяются он высоких широт к низким, меняя параметры поляризации. В этом представлении мы даем обзор этих недавних результатов, полученных от наблюдений на Дальнем Востоке России и в Японии..*

## 1. Introduction

In order to measure ionospheric/atmospheric disturbances and geomagnetic pulsations in the longitudes of Far-East Asia, we have newly installed two all-sky airglow imagers and two induction magnetometers at Stecolny near Magadan (MGD, 60.05N, 150.73E, November 4, 2008-) and Paratunka (PTK, 52.97N, 158.25E, August 17, 2007-). The stations are shown in Figure 1. The circles indicate the field-of-view of the airglow imagers (r=500 km). The induction magnetometers were installed at MGD, PTK, Moshiri (MSR, 44.37N, 142.27E, July 14, 2007-), and Sata (STA, 31.02N, 130.68E, September 5, 2007-). MGD and PTK are in the field-of-view of the SuperDARN Hokkaido radar which is located at Rikubetsu (RIK, 43.5N, 143.8E).

From these observations, several new results were obtained. In this presentation, we show some results regarding the medium-scale traveling ionospheric disturbances (MSTIDs) and Pc1 geomagnetic pulsations.

## 2. MSTID observations

Nighttime medium-scale traveling ionospheric disturbances (MSTIDs), which have horizontal-scale sizes of ~50-500 km and phase speeds of ~50-200 m/s, are frequently observed at middle latitudes. Recent statistical studies of two-dimensional MSTID images over Japanese and American sectors using 630-nm airglow imagers and total electron content (TEC) maps obtained by Global Positioning System (GPS) receivers indicate that they have a predominantly northwest-southeast phase surface and propagate southwestward [e.g., Garcia et al., 2000; Shiokawa et al., 2003; Kotake et al., 2006]. The ionospheric Perkins instability is a likely mechanism in generating these MSTIDs, since it can explain the northwest-southeast phase surface [Perkins, 1973]. However, the growth rate of the instability is too small to develop in the ordinary nighttime ionosphere at middle latitudes. Moreover, the instability cannot explain the observed systematic southwestward motion of MSTIDs.

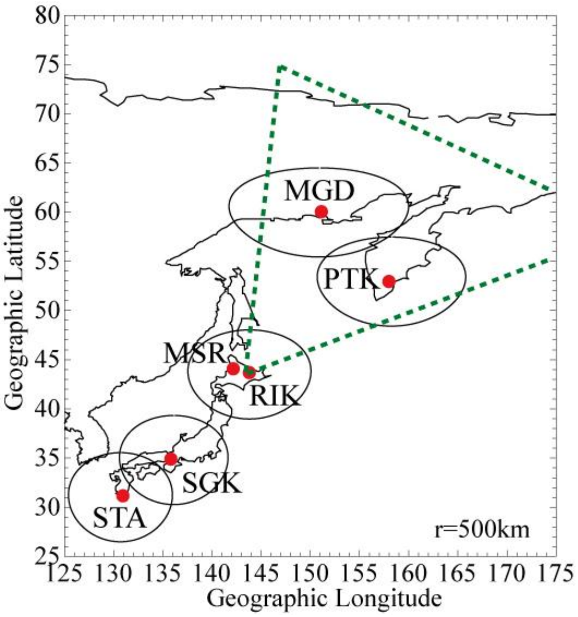


Figure 1. Stations of the all-sky airglow imagers, magnetometers, and the Hokkaido HF radar in Japan and Far-Eastern Russia. The circles and the triangle show the field of view of the airglow imager and the radar, respectively.

Using the SuperDARN HF radar at RIK, and the OI 630-nm airglow imager at PTK, Suzuki et al. (2009) and Koustov et al. (2009) investigated plasma drift in the MSTID wave phase surface. Figure 2 shows the phase relation between the MSTIDs in airglow (Figure 2a) and the radar Doppler velocity (Figure 2b) at 1100–1700 UT (2130–0330 LT) of December 8, 2007, together with the radar echo power (Figure 2c), as reported by Suzuki et al. (2009). The black lines in Figure 2 indicate the airglow enhancement phases identified from Figure 2a. At ~1220–1530 UT (2250–0200 LT), downward moving wavefronts of MSTIDs, indicating southwestward propagation, were clearly seen in all the RTI plots of the airglow intensity, Doppler velocity, and echo power. The wavefronts with airglow enhancement (depletion) showed a good agreement with the positive (negative) Doppler velocity and weaker (stronger) echo power phases, particularly at ~1230–1500 UT. These results indicate that the weaker (stronger) echo regions having positive (negative) Doppler velocities appeared in the airglow enhancement (depletion) region and moved in the same direction and with the same speed as the MSTIDs in the airglow images (i.e., southwestward at ~100 m/s). A similar phase relation between the optical and radar data was also identified from the RTI plots, which were made along other radar beams. From these correspondence MSTID phase surface in the airglow images and HF radar echoes, Suzuki et al. (2009) concluded that these polarity changes of plasma drifts are attributed to ExB plasma drifts caused by the polarization electric field embedded in the MSTIDs. They also suggested that the observed field-aligned irregularities (FAIs) that cause the HF radar echoes were generated by the gradient drift instability on the bottomside of the F region.

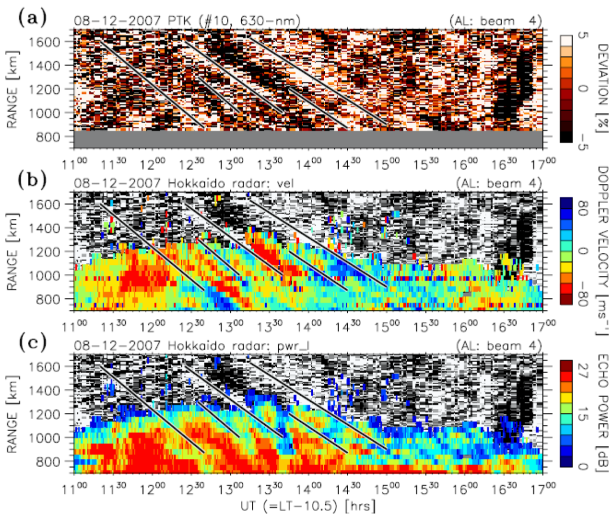


Figure 2. Range-time-intensity plots of (a) 630-nm airglow intensity, (b) Doppler velocity, and (c) radar echo power along beam 4 at 1100–1700 UT (2130–0330 LT at Paratunka) on 8 December 2007. The vertical axis represents the range from the Hokkaido radar to the detection point along the beam path. Airglow enhancements are traced by the black lines. (After Suzuki et al., 2009).

Using similar MSTID images in the 630-nm airglow, Shiokawa et al. (2008) found an interesting event of

MSTID motion change from southwestward to northeastward. Figure 3 shows a comprehensive summary of their MSTID event of August 19, 2007. The airglow deviation

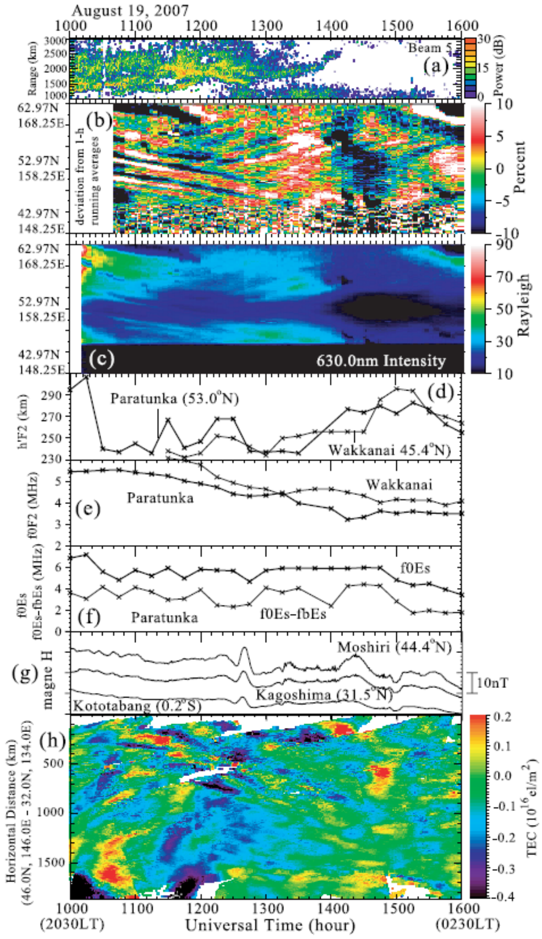


Figure 3. From top to bottom, (a) echo power obtained by the Hokkaido HF radar along beam 5, cross sections (keograms) of 630-nm airglow images along the northeast to southwest baseline for (b) deviation from 1-hour running averages and (c) absolute intensity, (d) ionospheric height (h'F2), (e) foF2, which corresponds to the F-layer peak electron density, (f) foEs and foEs-fbEs, obtained by ionosondes at PTK, and Wakkanai (45.4N, 141.7E, northern edge of Japan), (g) H component geomagnetic variations observed at MSR, Kagoshima (31.5N, 130.7E), and Kototabang (0.2S, 100.3E), and (h) cross section of GPS-TEC variations along the northeast to southwest baseline over Japan. (After Shiokawa et al., 2008).

keogram in Figure 3b clearly shows the turning of the MSTID motion from southwestward at 1000-1200 UT to northeastward afterwards. The turning point moves from the northeastern edge of the keogram at 1200 UT to lower latitudes at 1300 UT at the zenith of PTK. At lower latitudes below the zenith of PTK, the MSTIDs continue to propagate southwestward with a phase speed of ~100 m/s. At further lower latitudes in Japan, Figure 3h shows that the MSTIDs move southwestward continuously over 1100-1500 UT over the entire region of Japanese latitudes with a phase speed of ~70 m/s. The propagation of the turning point from the northeastern edge at 1200 UT to the zenith of Paratunka at 1300 UT in Figure 3b coincides with the enhancement of the 630-nm airglow intensity in Figure 3c, which also seems to propagate from the northeastern edge (top of Figure 3c) at 1200 UT to the zenith at 1300-1400 UT. The airglow intensity enhancement is not so clear around the zenith of PTK. Another airglow-enhanced region appeared at 1230-1400 UT in the southwest of PTK (at the bottom of Figure 3c). In Figure 3d, the F-layer virtual height (h'F2) at PTK suddenly decreased from 268 km (1230 UT) to 238 km (1245 UT), when the airglow enhancement reached near the zenith of PTK. This feature is consistent with the idea that the enhancement of the 630-nm airglow intensity was caused by the F-layer height decrease. The Hokkaido HF radar echoes in Figure 3a also confirm these F-layer height variations in the north of Japan. From these observations Shiokawa et al. (2008) suggested that the F-layer height decrease or the poleward thermospheric wind have some role in the MSTID propagation direction.

**3. Induction magnetometers**

Induction magnetometers can measure Pc1 pulsations of the geomagnetic field with a frequency range of 0.2-5 Hz. Pulsations in this frequency range usually remain undetected by fluxgate magnetometers due to their lower sampling rates and higher noise levels. Pc1 pulsations, which represent electromagnetic ion cyclotron (EMIC) waves in the inner magnetosphere, can be a loss mechanism of relativistic electrons in the outer radiation belt involving pitch-angle scattering of such electrons into the loss cone.

Figure 4 shows the examples of dynamic spectra of H-component magnetic field variations obtained by the induction magnetometers at five stations on February 27, 2009. Details of these magnetometers are given by Shiokawa et al. (2010). An intense PiB burst was observed at 0920-1300 UT at Athabasca (ATH, Canada, 54.7N, 246.7E) at a frequency range below 1 Hz, indicating substorm activity. At 1000-1030 UT, a clear enhancement of the power spectral density (PSD) was observed at MGD, PTK, and MSR at a frequency range of 0.1-2 Hz. Since the peak frequency tends to increase with time, it is likely that this Pc1 pulsation event corresponds to the intervals of pulsations of diminishing periods (IPDP) associated with the EMIC waves generated by ring current ions in the magnetospheric equatorial plane, which are in turn associated with the substorm at 0910 UT. The corresponding enhancement of the PSD can also be recognized at STA in the same interval at 1000-1030 UT, albeit with weaker intensity, even though the data at STA are affected by strong broadband noise at 1-10 Hz. The spectra at PTK are also affected by spiky noise, probably from nearby facilities in the observatory. These Pc1 observations were continuously made at these stations and analysis of their polarization parameters are under way.

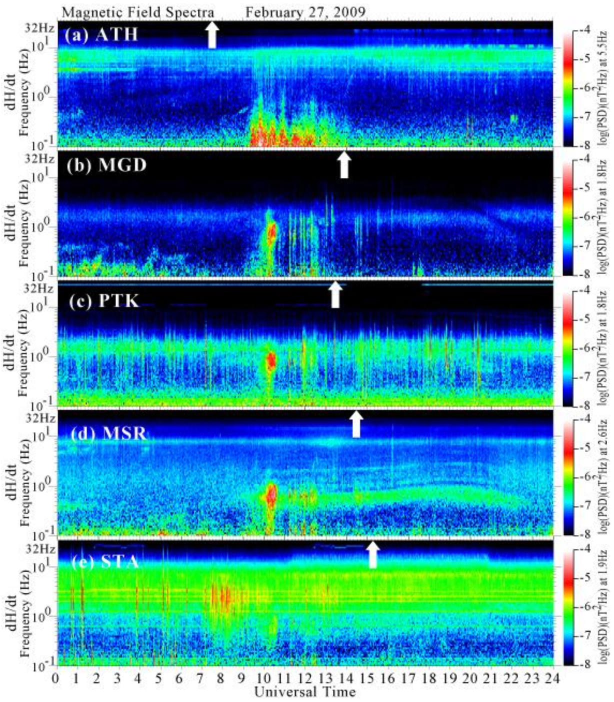


Figure 4. Dynamic spectra of the H component of the magnetic field fluctuations at 0.1-32 Hz as observed on February 27, 2009 at the five stations from higher (top) to lower (bottom) latitudes. The unit of power spectral density (PSD) in the color scale is calculated at the peak sensitivity of each station. The local midnight at each station is indicated by a white arrow. (After Shiokawa et al., 2010).

**4. Concluding Remarks**

The measurements by all-sky airglow imagers and induction magnetometers at Far-Eastern Russia and Japan have been continued since 2007 toward the solar maximum. The quick-look plots of data obtained by these instruments are opened at the homepage at http://stdb2.stelab.nagoya-u.ac.jp/omti/ (for imagers) and at http://stdb2.stelab.nagoya-u.ac.jp/magne/ (for magnetometers). Not only for analysis of each station data, these measurements at latitudinal chain stations will be also useful to elucidate the energy propagation mechanisms from high-latitude auroral zone to low latitudes, such as large-scale TIDs during geomagnetic storms and propagation of MHD waves in the ionospheric duct.

**Acknowledgments**

This work was carried out under an agreement between IKIR and STEL on the international project "Ground and Satellite Measurements of Geospace Environment in the Far Eastern Russia and Japan". This work was supported by Grants-in-Aid for Scientific Research (16403007, 18403011, 19403010, and 20244080), the 21th Century COE Program (Dynamics of the Sun-Earth-Life Interactive System, No.~G-4), the Global COE Program of Nagoya University "Quest for Fundamental Principles in the Universe (QFPU)", and the Special Funds for Education and Research (Energy Transport Processes in Geospace) from MEXT, Japan.

**References**

1. Garcia, F. J., M. C. Kelley, J. J. Makela, and C.-S. Huang, Airglow observations of mesoscale low-velocity traveling ionospheric disturbances at midlatitudes, *J. Geophys. Res.*, *105*, 18,407-18,415, 2000.
2. Kotake, N., Y. Otsuka, T. Tsugawa, T. Ogawa, and A. Saito, Climatological study of GPS total electron content variations caused by medium-scale traveling ionospheric disturbances, *J. Geophys. Res.*, *111*, A04306, 10.1029/2005JA011418, 2006.
3. Koustov, A., N. Nishitani, K. Shiokawa, S. Suzuki, and B.M. Shevtsov, Joint observations of a traveling ionospheric disturbance with the Paratunka OMTI camera and the Hokkaido HF radar, *Ann. Geophys.*, *27*, 2399-2406, 2009.
4. Perkins, F., Spread F and ionospheric currents, J. Geophys. Res., 78, 218-226, 1973.
5. Shiokawa, K., C. Ihara, Y. Otsuka, and T. Ogawa, Statistical study of nighttime medium-scale traveling ionospheric disturbances using midlatitude airglow images, *J. Geophys. Res.*, *108(A1)*, 1052, doi:10.1029/2002JA009491, 2003.
6. Shiokawa, K., Y. Otsuka, N. Nishitani, T. Ogawa, T. Tsugawa, T. Maruyama, S. E. Smirnov, V. V. Bychkov, and B. M. Shevtsov, Northeastward motion of nighttime medium-scale traveling ionospheric disturbances at middle latitudes observed by an airglow imager, *J. Geophys. Res.*, *113*, A12312, doi:10.1029/2008JA013417, 2008.
7. Shiokawa, K., R. Nomura, K. Sakaguchi, Y. Otsuka, Y. Hamaguchi, M. Satoh, Y. Katoh, Y. Yamamoto, B. M. Shevtsov, S. Smirnov, I. Poddelsky, and M. Connors, The STEL induction magnetometer network for observation of high-frequency geomagnetic pulsations, *Earth Planets Space, in press*, 2010.
8. Suzuki, S., K. Hosokawa, T. F. Shibata, K. Shiokawa, Y. Otsuka, N. Nishitani, T. Ogawa, A. V. Koustov, and B. M. Shevtsov, Coordinated observations of nighttime medium-scale traveling ionospheric disturbances in 630-nm airglow and HF radar echoes at midlatitudes, *J. Geophys. Res.*, 114, A07312, doi:10.1029/2008JA013963, 2009.